Comparison of SUV to Whole Body Restricted Diffusion – A study using simultaneous PET-MRI in patients with cancer

Ronald Borra[1], Shanaugh McDermott[2], Onofrio Catalano[3], Ciprian Catana[1], Bruce R Rosen[1], and Alexander R. Guimaraes[1,2]

[1]*Radiology; Massachusetts General Hospital, Martinos Center for Biomedical Imaging, Charlestown, MA, United States,* [2]*Radiology, Massachusetts General Hospital; Division of Abdominal Imaging and Interventional Radiology, Boston, MA, United States,* [3]*Radioloy, Naples General Hospital, Naples, Naples, Italy*

Introduction

Positron emission tomography (PET) with ^{18}F-fluoro-2-deoxy-D-glucose (FDG) is an indirect measure of metabolic activity and is a mainstay of staging various malignancies including lymphoma, esophageal, lung, rectal and cervical cancer. In many oncologic subtypes, including lung cancer and lymphoma, standardized uptake value (SUV), a measure of tumor glucose metabolic activity, has shown prognostic value in addition to being a measure of therapeutic efficacy. [1, 2] FDG-PET/CT, however, involves radiation exposure, which is a concern for younger populations afflicted with malignancy, and FDG avidity is dependent on tumor type with many tumor types having variable FDG avidity (e.g. pancreatic cancer, carcinoid). [3]

Whole body magnetic resonance imaging (wbMRI) has the ability of measuring metabolic activity, functional information (e.g. DCE-MRI), with higher soft-tissue contrast than CT, making it the method of choice for local staging of various malignancies within the liver, and male and female pelvis. In addition, and perhaps most importantly, malignancies have increased cellularity. Diffusion weighted imaging (DWI) has the ability of visualizing random Brownian motion within tissues. By having a predictable, exponential signal decrement, DWI has the ability of quantifying the apparent diffusion coefficient (ADC). As a result, malignant tumors, many of which share high cellularity, have demonstrated restricted diffusion and lower ADC than nearby tissues. [4] As a result, DWI has played an increased role in the grading and staging of malignancies.

Although it is clear that FDG-PET is a biomarker of metabolism, and wbDWI may be a biomarker of increased cellular density, both are currently being used as biomarkers of malignancy. Yet, the correlation of SUV to ADC, both subjectively, and quantitatively has shown remarkable variance with some publications demonstrating high correlation, and others showing none at all. [5-12] The recent advent of simultaneous whole-body PET-MRI with the Siemens Biograph mMR (Siemens Healthcare, Erlangen, Germany), allows us to test the hypothesis directly whether there is a correlation between SUV and ADC. In this abstract, we chose to study this in 26 patients with different oncologic diagnoses undergoing PET-MRI on the same day as a clinical PET-CT examination.

Methods

Study participants. Subjects (n=26) with different oncologic diagnoses were enrolled and provided informed consent in this IRB approved study. Exclusion criteria included 18>age>80yrs and known contraindications to MRI (e.g. metallic implants, etc.).

MR imaging. The Biograph mMR 3T scanner was used for these studies. Specially fabricated PET-compatible phased array coils (6-channel) were used to acquire the MR data. A 2-point Dixon 3D VIBE breath-hold T1 weighted sequence using the following parameters (iPAT factor 2, TR 3.6ms, TE1 1.225ms, TE2 2.45ms, matrix size 79x192, NEX=1, FOV 500mm, slice thickness, 5.5mm, flip 10) was used to derive the attenuation correction (AC) map. This manufacturer-provided method allows the identification of four tissue types (fat, soft tissue, lung, background). Being difficult to segment from the MR data, bone tissue is treated as soft tissue for AC purposes. wbDWI was performed using a single shot echo planar imaging technique (SSEPI) using the following parameters (iPAT factor 2, FOV 420, matrix 112x156, slice thickness 6, NEX 2, TE 68ms, TR 7800, TI 220ms (fat suppression), with b values including (0,50,800)).

PET imaging. PET data were acquired using shallow free breathing from the upper thighs cephalad. 4-5 bed positions (bp) were required to cover the entire abdomen and pelvis with ~10 min/bp. PET axial field of view was 25.8cm. PET data were reconstructed using a 3D AW OSEM, with 3 iterations and 21 subsets, zoom =1, and Gaussian smoothing of 4mm FWHM.

Data analyses. Image analysis was performed using OsiriX (OsiriX, Geneva, Switzerland) software with fusion software embedded. Region of interest (ROI) analysis was performed on FDG-PET data, demonstrating avidity 1SD above liver or mediastinum, fused with axial DWI data. Analysis of DWI data included visibility of lesion on DWI data at b=50 and 800, in addition to quantitative measures of SUV as compared to ADC values. Lesions were then divided into 3 different anatomic regions (thorax, abdomen, skeleton). SUV_{max} was compared to ADC_{min} using linear regression and compared amongst all data, and for each body region. In addition, ADC_{min} data was categorized as restricted (R) or non-restricted (NR) based on two different threshold values (ADC 1000 or ADC 1500), both of which supported by literature [5-12]. Based on these thresholds, an unpaired two-tailed t-test was used for comparisons using GraphPad Prism 5 (GraphPad Software, La Jolla, CA,). $P \leq 0.05$ was considered statistically significant.

Results

Within the 26 subjects analyzed, there were 80 FDG avid lesions, 58 of which were visualized on DWI. The 22 lesions "missed" were equally distributed amongst all 3 body regions with FDG SUVs ranging from 3.4-13.1. Figure (a) illustrates wbDWI as compared to (b) FDG-PET images in a patient with a large left upper lobe mass that demonstrates concordant FDG avidity and ADC restriction, in addition to other foci of activity, some of which are concordant (arrowhead) and others are discordant (red arrow). Figure (c) demonstrates scatterplots comparing restricted (R) and non-restricted (NR) as determined from an ADC threshold (ADC<1500 (top)) and (ADC<1000 (bottom)) without a significant difference in SUV comparing these two subsets ($p<0.5$). Figure (d) correlates ADC_{min} vs. SUV_{max} for all tumors (R^2 0.03), and then within the abdomen (R^2 0.3), and thorax (R^2 0.004). Linear regression demonstrates no correlation but an inverse trend.

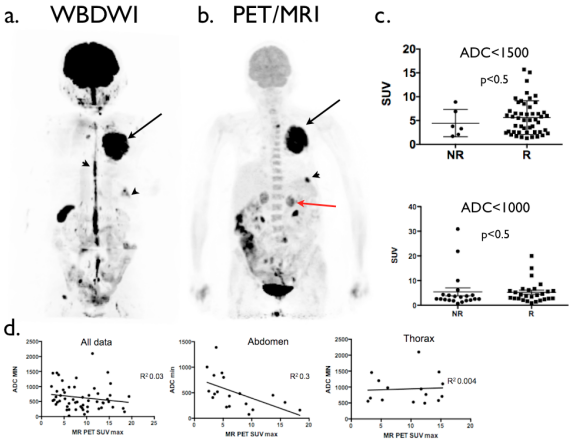

Figure - a) wbDWI acquired on the Biograph mMR scanner demonstrating a patient with a large mass in the left upper lobe (arrow), and multiple other foci of restricted diffusion (arrowhead). b) FDG-PET MIP image demonstrating a concordant FDG-avid left upper lobe mass (arrow) and concordant FDG-avid/restricted diffusion lesion (arrowhead), but discordant adrenal gland metastases (red arrow). c) Plot demonstrating the scatter of non-restricted (NR) and restricted (R) lesions with a threshold of (ADC<1500 (top)) and (ADC<1000 (bottom)). Figure (d) correlates ADC_{min} vs. SUV_{max} for all tumors (R^2 0.03), and then within the abdomen (R^2 0.3), and thorax (R^2 0.004).

Conclusions

Both DWI and FDG PET are biomarkers of malignancy albeit measuring different physiologic or structural parameters. When comparing directly FDG avid lesions with ADC restriction, there is no correlation. When comparing quantitative ADC vs. SUV, there is a linear trend, with significant scatter, however. Our data support that thoracic DWI remains an area for technique improvement. Although both FDG and DWI can be used as biomarkers of malignancy, the lack of concordance in these data support further, more extensive experiments in how to use the combined measures of restricted diffusion and FDG avidity in each malignant subtype.

References

1. Kinahan, P. E. (2010). Semin Ultrasound CT MR **31**:496-505
2. Wahl, R. L. et al. (2009). J Nucl Med **50 Suppl 1**:122S-150S
3. Kwee, T. C. et al. (2011). Eur J Nucl Med Mol Imaging **38**:1158-1170
4. Padhani, A. R. (2009). Neoplasia **11**:102-125
5. Choi, B. B. et al. (2012). World J Surg Oncol **10**:126
6. Ho, K. C. et al. (2009). Eur J Nucl Med Mol Imaging **36**:200-208
7. Ippolito, D. et al. (2012). Abdom Imaging
8. Matsushima, N. et al.(2012). Ann Nucl Med **26**:262-271
9. Mori, T. et al. (2008). J Thorac Oncol **3**:358-364
10. Nakajo, M. et al. (2012). Clin Nucl Med **37**:475-480
11. Nakamatsu, S. et al. (2012). Clin Imaging **36**:90-97
12. Regier, M. et al. (2012). Eur J Radiol **81**:2913-2918